Structure, Vol. 13, 963–971, July, 2005, ©2005 Elsevier Ltd All rights reserved. DOI 10.1016/j.str.2005.04.016

Obligate Heterodimerization of the Archaeal Alba2 Protein with Alba1 Provides a Mechanism for Control of DNA Packaging

Clare Jelinska,[1] Matthew J. Conroy,[2] C. Jeremy Craven,[2] Andrea M. Hounslow,[2] Per A. Bullough,[2] Jonathan P. Waltho,[2] Garry L. Taylor,[1] and Malcolm F. White[1,*]

[1]Centre for Biomolecular Science
University of Saint Andrews
North Haugh, Saint Andrews
Fife KY16 9ST
United Kingdom

[2]Department of Molecular Biology and Biotechnology
University of Sheffield
Firth Court, Western Bank
Sheffield S10 2TN
United Kingdom

Summary

Organisms growing at elevated temperatures face a particular challenge to maintain the integrity of their genetic material. All thermophilic and hyperthermophilic archaea encode one or more copies of the Alba (Sac10b) gene. Alba is an abundant, dimeric, highly basic protein that binds cooperatively and at high density to DNA. *Sulfolobus solfataricus* encodes a second copy of the Alba gene, and the Alba2 protein is expressed at 5% of the level of Alba1. We demonstrate by NMR, ITC, and crystallography that Alba2 exists exclusively as a heterodimer with Alba1 at physiological concentrations and that heterodimerization exerts a clear effect upon the DNA packaging, as observed by EM, potentially by changing the interface between adjacent Alba dimers in DNA complexes. A functional role for Alba2 in modulation of higher order chromatin structure and DNA condensation is suggested.

Introduction

The nucleosome is the universal unit for DNA organization and compaction in the eukarya. Prokaryotic chromatin structure and organization, however, is more diverse and less well understood. Prokaryotes have to compact their DNA by over 1000-fold (Wu, 2004), and utilize a wide variety of DNA binding proteins in their chromatin. Bacterial chromatin proteins, such as HU, IHF, Fis, and H-NS, interact with DNA in a variety of ways (Wu, 2004). The archaeal DNA replication and transcription pathways are strikingly similar to those in eukarya and quite different from the equivalent bacterial processes (Keeling and Doolittle, 1995). It is, therefore, not surprising that archaeal chromatin proteins are in large part different from those found in bacteria. Most euryarchaea have true histone proteins, which are organized into tetrameric nucleosomes that wrap DNA (Sandman et al., 2001), but these are lacking in the *Thermoplasmas* and the crenarchaea (White and Bell, 2002). Arguably the most widespread archaeal chromatin protein is Alba, also known as Sac10b or Sso10b. Alba is abundant, representing 4% of the total protein in *Sulfolobus shibatae* (Xue et al., 2000), and is present in the genome sequences of every archaeal species that has a thermophilic or hyperthermophilic lifestyle. The correlation of Alba with growth at elevated temperatures hints at a role for Alba in DNA protection and stability under these conditions, as high temperatures lead to increased rates of DNA damage and thermal melting of duplexes.

Alba is a homodimer in solution, with subunits adopting a mixed α/β fold similar to that of the bacterial translation initiation factor IF3 C-terminal domain (Wardleworth et al., 2002). Distant relationships with other ribonucleoproteins in archaea and eukarya have prompted the suggestion that Alba may have originated as an RNA binding protein (Aravind et al., 2003). Indeed, Alba binds RNA and DNA with similar affinity in vitro, and may also have a role as an RNA chaperone in vivo (Guo et al., 2003). The Alba dimer has a highly basic surface that is presumed to constitute the main DNA binding interface, and this has been confirmed by mutational studies (Bell et al., 2002; Wardleworth et al., 2002). In *Sulfolobus solfataricus*, Alba is reversibly acetylated on a single lysine residue, Lys16, which forms part of the DNA binding interface (Marsh et al., 2005).

Alba binds dsDNA cooperativity, with an apparent dissociation constant in the nanomolar or low micromolar range (Wardleworth et al., 2002). The Alba protein can constrain negative DNA supercoils at high temperatures, consistent with a role in DNA packaging (Xue et al., 2000). DNA is bound with an initial stoichiometry of 12 bp per Alba dimer, followed by a high-density binding form in which the stoichiometry approaches 6 bp per dimer (Wardleworth et al., 2002; Xue et al., 2000). Electron microscopy (EM) studies of purified Alba protein from *Sulfolobus acidocaldarius* in complex with plasmid DNA have shown that two DNA duplexes can be interwound by Alba at subsaturating protein concentrations (Lurz et al., 1986). At higher protein concentrations, a single DNA duplex was bound, with little compaction of the DNA evident. The authors proposed a model with two helical protein fibers wound around one or two DNA duplexes (Lurz et al., 1986).

Six of the sequenced archaeal genomes have two copies of the Alba gene (Figure 1A). Phylogenetic reconstruction suggests that gene duplication has been a relatively recent event in species such as *Archaeoglobus fulgidus* and *Methanococcus kandlerii*, in which the two copies present are closely related to one another (Figure 1A). However, in the *Sulfolobales*, gene duplication appears to have been followed by rapid divergence of the duplicated gene. We define the gene encoding the more highly conserved Alba sequence as the Alba1 gene, and the gene encoding the more divergent sequence as Alba2. The Alba1 proteins from *Sulfolobus solfataricus*, *S. tokodaii*, and *S. acidocaldarius* are over 90% identical to one another and about 60% identical to Alba1 sequences from more divergent archaea.

*Correspondence: mfw2@st-and.ac.uk

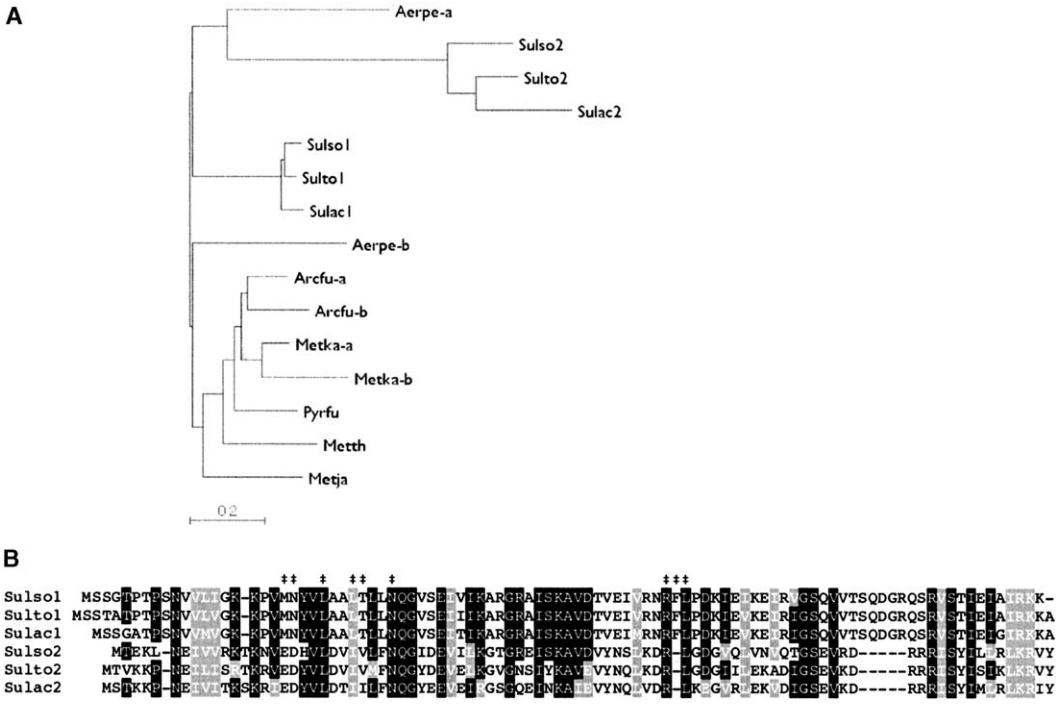

Figure 1. Protein Sequence Analysis of Archaeal Alba Proteins

(A) Phylogenetic tree showing duplication of the Alba gene in different lineages. A midpoint rooted, neighbor joining tree with Poisson correction and proportional gap distribution, generated using a distance matrix algorithm (MacVector). Branch lengths are drawn proportionally to the number of differences between each sequence (p-distance). All sequences were obtained from Swissprot with the exception of those from *Sulfolobus acidocaldarius*, which were a personal communication from Roger Garrett. Aerpe, *Aeropyrum pernix*; Sulso, *Sulfolobus solfataricus*; Sulto, *Sulfolobus tokodaii*; Sulac, *Sulfolobus acidocaldarius*; Thevo, *Thermoplasma volcanium*; Metth, *Methanothermobacter thermautotrophicum*; Arcfu, *Archaeoglobus fulgidus*; Metka, *Methanococcus kandleri*; Pyrfu, *Pyrococcus furiosus*; Metja, *Methanococcus janaschii*.

(B) Sequence alignment of Alba1 and Alba2 from three *Sulfolobus* species, showing identical and similar residues in black and gray, respectively. Residues associated with a conserved tetramer interface in the Alba1 crystal structure are denoted by ‡.

However, *Sulfolobus* Alba2 sequences are only 30%–40% identical to Alba1 sequences from the same species, and are 60%–70% identical to one another (Figure 1B). This suggests that the *Sulfolobus* Alba2 protein has diverged, possibly toward a novel function, but in the absence of biochemical or genetic studies this role has been unclear. The *Sulfolobus solfataricus* Alba2 (Sso10b2) protein has been crystallized, and has a similar structure to Alba1 (Chou et al., 2003). Here we show that Alba2 is expressed at a lower level than, and forms obligate heterodimers with, Alba1. The Alba1:Alba2 heterodimer has been crystallized, and we demonstrate a potential role for Alba2 in the control of DNA packaging.

Results

Expression and Purification of Native Alba Proteins

Both Alba proteins are expressed in *Sulfolobus solfataricus*, and we estimate that Alba2 is expressed in vivo at ~5% of the level of Alba1 in stationary phase (Figure 2A). However, despite having significantly different isoelectric points (Alba1 and Alba2 have pIs of 11 and 8.5, respectively), the two proteins coeluted from a cation exchange column. Partial resolution of Alba proteins was achieved using Mono-S cation exchange chromatography (Figure 2B). Native Alba1 is uniformly acetylated at the N terminus and can be reversibly acetylated at lysine 16 (Wardleworth et al., 2002). A pure sample of diacetylated Alba1 (Ac-Alba) was obtained, as this form of the protein is predominant and elutes first from the column (Bell et al., 2002). A single mass-ion was identified for Alba2 (m/z = 10,151) by MALDI-TOF mass spectrometry, corresponding to a singly (probably N-terminal) acetylated form of the protein (Figure 2B). Coelution of Alba1 and Alba2 during purification suggested that the proteins interact with one another. This was confirmed by hydroxyapatite chromatography, through which it was found that a mixture of the two proteins coeluted at a phosphate concentration intermediate to those of the individual pure proteins (Figure 2C).

Alba Heterodimer Formation

The nature of the interaction between Alba1 and Alba2 was investigated using ^{1}H-^{15}N HSQC NMR spectroscopy. The intensities of slow exchange peaks (Figure 3A), observed as a solution of ^{15}N-labeled Alba1 titrated with unlabeled Alba2, were found to increase proportionally to completion at a 1:1 stoichiometry. The

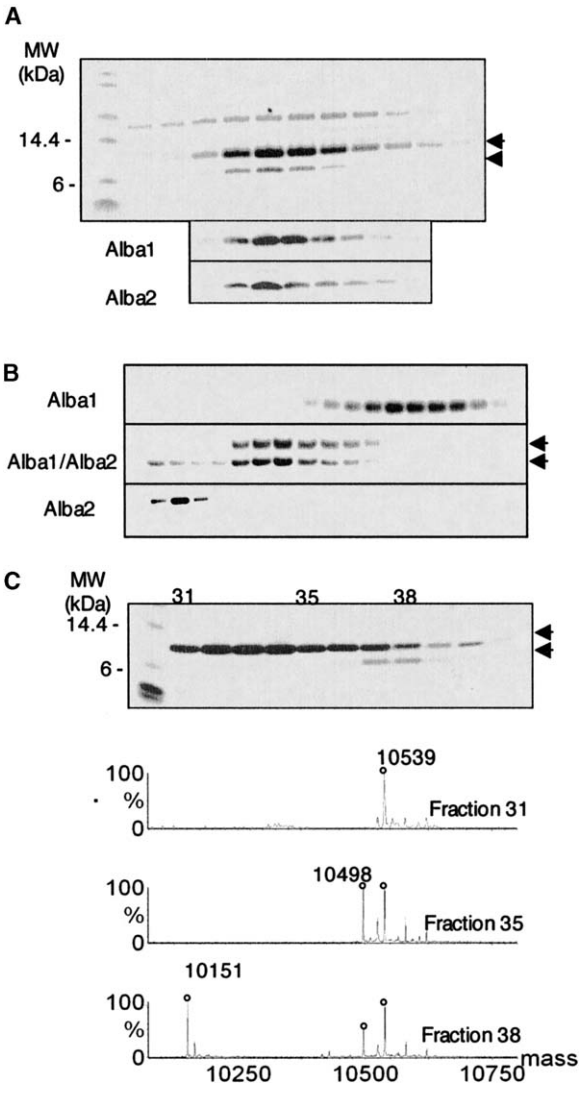

Figure 2. Copurification Of The Alba1 and Alba2 Proteins

(A) SDS-PAGE of fractions containing native Alba proteins from initial purification of *Sulfolobus solfataricus* cell extract by Resource cation exchange chromatography. For all gels shown, lanes correspond to fractions eluting at progressively higher ionic strength, and arrows indicate Alba1 (upper) and Alba2 (lower). The corresponding Western blots, exposed to polyclonal antibodies obtained from antiserum raised against the pure recombinant proteins, selectively confirm the presence of both Alba1 and Alba2.

(B) Recombinant Alba1 (top panel) elutes from a hydroxyapatite column significantly later than recombinant Alba2 (bottom panel). However, the pure proteins coelute when mixed together (middle panel), suggesting a stable interaction.

(C) SDS-PAGE of native Alba proteins purified by Mono S cation exchange chromatography. Fractions that were analyzed by MALDI-TOF mass spectrometry are indicated and the spectra are shown below. All three fractions have a peak at 10,539 Da, corresponding to diacetylated Alba1. Fraction 35 has an additional peak at 10,498, corresponding to monoacetylated Alba1, and fraction 38 has a peak at 10,151 Da, corresponding to monoacetylated Alba2.

changes in chemical shift are shown in Figure 3B. When superimposed onto the Alba crystal structure, it became apparent that the shift changes were localized to the main dimer interface, indicating the formation of a heterodimer (Figure 3C). From the signal-to-noise ratio measured at a 1:1 stoichiometry of Alba1:Alba2 in the ^{1}H-^{15}N HSQC NMR spectrum, it is clear that the overwhelming majority (>99%) of Alba1 and Alba2 are present as heterodimer. A strong interaction between Alba1 and Alba2 was confirmed using isothermal titration calorimetry (ITC) at 55°C. As Alba1 was titrated into Alba2, a highly exothermic interaction was observed (Figure 3D). Due to the high affinity of this interaction, it was not possible to obtain an accurate value for the dissociation constant, although an enthalpy change corresponding to −4.1 kcal mol^{-1} of heterodimer was measured directly. When pure, the individual proteins appear as dimers by gel filtration at 50 μM, and there is no evidence of dissociation of either homodimer by ITC upon dilution from 50 to 0.03 μM (data not shown). Therefore, we assume that the individual dissociation constants for the homodimers are <10 nM. In a numerical simulation of the equilibrium between two homodimers and a heterodimer, we found that the amount of heterodimer present can be accurately described as a function of the ratio of the three defining equilibrium constants, providing that the total concentrations of both species greatly exceeds the highest dissociation constant (>10^3 higher). As the cellular concentration of Alba1 may be as high as 500 μM (Xue et al., 2000), this would suggest an in vivo concentration for Alba2 of the order of 25 μM. The approximation can then be extended to biological conditions in which our simulated data show that Alba2 will exist overwhelmingly in the heterodimeric form. For a detailed discussion of Alba heterodimerization, see the Supplemental Data, available with this article online.

Alba Heterodimer Crystal Structure

The preponderance of heterodimer at a 1:1 ratio of Alba1:Alba2 facilitated crystallization, and we have solved the structure of a trigonal crystal form to 1.7 Å (PDB accession number 2bky). Superimposition of Alba1 and Alba2 monomers from the relevant homodimer and heterodimer crystal structures shows that the extended β-hairpin regions of both proteins undergo the largest conformational changes (Figure 4). As these regions are probably flexible in solution (Chou et al., 2003; Wardleworth et al., 2002), the differences are likely to be artifacts of crystal packing interactions. A comparison with the NMR data shows that this is indeed the case for Alba1, as no chemical shift changes were measured in this region upon mixing with Alba2. Due to the large number of factors involved in stabilizing protein-protein interfaces, it is inherently difficult to derive parameters with which to assess or explain differences in stability. A comparison of Alba dimer interactions exemplifies this (Table S1). In fact, as our numerical simulation shows that extensive heterodimerization depends only on the *ratio* of the three equilibria, it does not imply that the heterodimer must be more stable than *both* homodimers (Supplemental Data).

DNA Binding Affinity and Cooperativity

To establish a functional role for the heterodimer, we first measured binding affinities of the various forms of

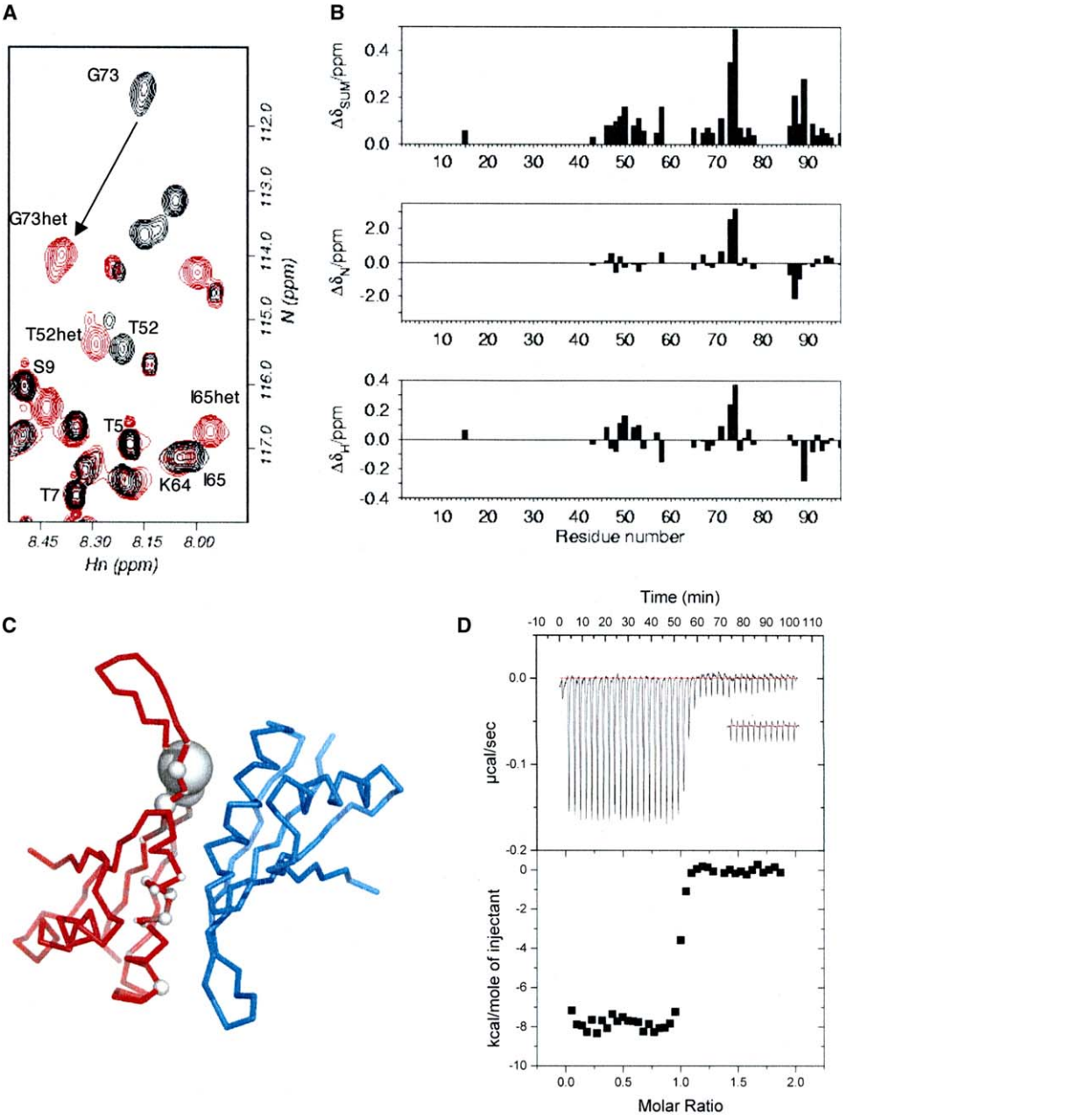

Figure 3. Heterodimerization of Alba1 and Alba2

(A) A region of the overlaid ^{1}H-^{15}N HSQC spectra of Alba1 in the Alba1 homodimer (black) and at a 1:1 ratio of Alba1:Alba2 (red). Cross-peak assignments are shown for selected residues, where "het" is appended to heterodimer assignments.

(B) Plots of chemical shift changes against residue number. Data are shown for nitrogen shifts, proton shifts, and as a weighted combination of the two ($\sqrt{[(dn/10)^2+dnh^2]}$).

(C) The ca trace for a preliminary heterodimer model, constructed from the crystal structure of Alba1 (Wardleworth et al., 2002) by superimposing a monomer of Alba2 (from the Alba2 crystal structure [Chou et al., 2003]) onto one monomer of Alba1. Alba1 is in red and Alba2 is in blue. The spheres on the Alba1 monomer represent the chemical shift changes observed on formation of the heterodimer (Figure 3B). The radii of the spheres are proportional to the weighted sum chemical shift change.

(D) Heterodimer formation observed by isothermal titration calorimetry at 55°C. The heat released upon titration of a solution of Alba2 with aliquots of Alba1 in the same buffer is shown. Background signals measured upon injection of Alba1 into buffer and buffer into Alba2 were subtracted from the data (inset). The processed data indicate strong binding and, therefore, only the enthalpy change of –4.1 ± 0.1 kcal mol^{-1} could be determined, as this is measured directly.

Alba with 16 and 39 bp duplexes by electrophoretic DNA mobility shift assay (Table 1 and Figure 5). The Alba2 homodimer binds DNA with a 10- to 20-fold lower affinity than the Alba1 homodimer, suggesting that Alba2 has an inherently weaker DNA binding affinity than Alba1. However, the physiologically relevant Al-

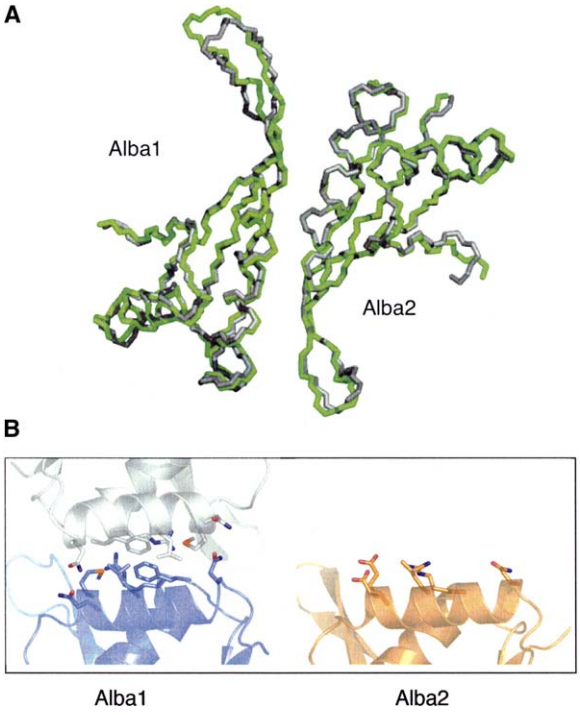

Figure 4. Crystal Structure of the Alba Heterodimer

(A) The heterodimer crystal structure, shown in green, is superimposed onto monomers from the respective homodimer crystal structures, shown in gray. Backbone n, ca, and c′ atoms are represented as sticks.

(B) Comparison of the conserved dimer:dimer interface found in Alba1 homodimer crystal structures (Wardleworth et al., 2002; Zhao et al., 2003) with the corresponding region of Alba2. Secondary structure elements are shown in cartoon form where one Alba1 dimer is shown in white, the other in blue, and the Alba2 dimer is shown in orange. The side chains of Alba1 interface residues (M20, N21, L24, N31, R59, and F60) and equivalent residues of Alba2 (D17, E18, L21, N28, and R56) are shown as sticks, where nitrogen, oxygen, and sulfur atoms are colored blue, red, and orange, respectively.

ba1:Alba2 heterodimer binds DNA duplexes with approximately the same affinity as the native Alba1 homodimer (Ac-Alba1). This suggests that the role of Alba2 is not directly associated with changes in the dissociation constant for DNA.

The acetylated and nonacetylated forms of Alba1 show only a 3- to 4-fold difference in binding affinity—a smaller difference than reported previously but consistent with results from other laboratories (Guo et al., 2003). The disparity is probably due to overestimation of the native Ac-Alba1 concentration in previous studies arising from the low extinction coefficient of the protein. Such a difference in DNA binding affinity would not be biologically important unless acetylation affects cooperativity during chromatin assembly, in which case small differences may have a significant cumulative effect when binding to longer duplexes. Indeed, it has been suggested that the specific acetylation of Alba affects protein oligomerization for optimal binding to DNA (Zhao et al., 2003). Our results indicate that differences in affinity between recombinant Alba1, Ac-Alba1, and the heterodimer remain relatively constant for 16 and 39 bp duplexes (Table 1). The affinity of recombinant Alba1 for the 39 bp duplex is also comparable to that found upon binding to longer duplexes (Xue et al., 2000). It therefore seems probable that the specific acetylation of lysine 16 functions as a molecular signal to other proteins rather than as a direct modulation of DNA binding affinity.

EM of Nucleoprotein Filaments

Previous EM studies of Alba:DNA complexes have revealed the formation of nucleoprotein filaments (Lurz et al., 1986). To further this revelation, we carried out a comparative EM study of Alba1 homodimer and Alba1:Alba2 heterodimer forms bound to relaxed, circular phiX174 plasmid DNA (Figure 6). For the Alba1 homodimer, open circular filaments with widths of 11.7 ± 1.1 nm (mean ± SEM) were observed at protein:DNA ratios of 6 bp/dimer. These must correspond to single plasmid molecules (i.e., one duplex) complexed with protein. At lower protein:DNA ratios of 12 bp/dimer, rather more "tangled" structures were observed, often showing "stem-loop" structures, in which the loop is clearly a single unbound duplex (~2 nm wide) at the end of a stem comprised of two duplexes wound together by protein. We also interpret many of these structures as originating from individual plasmid molecules. Interestingly, filaments incorporating two duplexes have the same width as those incorporating one and appear to have the same overall structure. These data are consistent with previous observations (Lurz et al., 1986). Published biochemical data on the interaction of Alba1 with DNA also suggest that an initial stoichiometry of 12 bp/dimer is reached, followed by a further binding event, to reach 6 bp/dimer (Wardleworth et al., 2002; Xue et al., 2000). Thus, all the data support the existence of two forms of DNA:protein complex formed by Alba1 at different stoichiometries.

Table 1. DNA Binding Affinities

	16 bp Duplex		39 bp Duplex	
Protein	Apparent K_d, nM	m[a]	Apparent K_d, nM	m[a]
Rec-Alba1	200 ± 4	1.3 ± 0.1	56 ± 2	1.9 ± 0.1
Ac-Alba1	720 ± 30	1.4 ± 0.1	150 ± 4	2.6 ± 0.1
Heterodimer	610 ± 20	1.8 ± 0.1	190 ± 6	3.4 ± 0.3
Alba2	6100 ± 2600	2.0 ± 0.1	1100 ± 60	1.5 ± 0.1

Values are mean ± SEM.

[a]This parameter was used during curve fitting to improve the fit, and reflects the steepness of the curves due to cooperative DNA binding by Alba. However, this is not a formal measure of cooperativity.

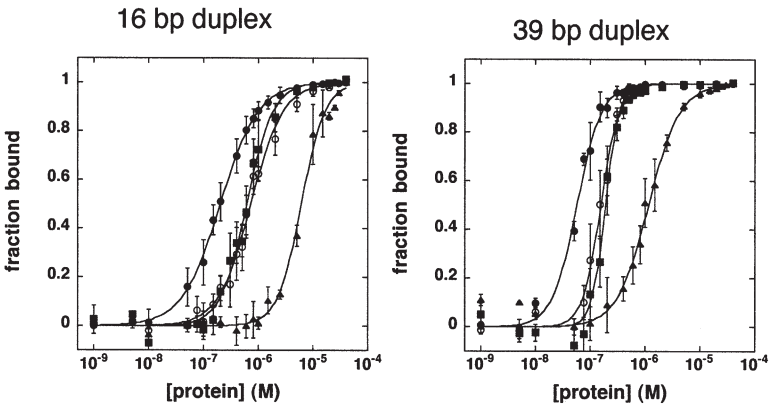

Figure 5. Alba-DNA Binding Curves Obtained by Gel Electrophoretic Retardation Analysis

Recombinant Alba1, recombinant Alba2, heterodimer, and Ac-Alba1 are denoted by filled circles, filled triangles, filled squares, and open circles, respectively. Standard error bars are shown together with curves obtained by fitting the data to the binding equation described in the text. A cooperative element to DNA binding by Alba is demonstrated both by increases in slope (m) and apparent binding affinity (K_d) observed for the 39 bp duplex when compared to the 16 bp duplex (Table 1).

At a ratio of 12 bp/dimer, the heterodimer formed filaments incorporating two DNA duplexes with seemingly identical properties to those of the homodimer filaments (Figure 6, lower right panel). However, at the higher protein:DNA ratio, significant differences were consistently observed. Under these conditions, the open circular plasmid complexes seen with Alba1 were never observed. Instead, highly branched, condensed complexes were always formed (Figure 6, top right panel), all of which contain two DNA duplexes. There thus appear to be significant differences between the DNA complexes formed at high protein concentrations with heterodimers compared to homodimers. This may relate to the differences seen in the conserved dimer:dimer interface of Alba1, which is not well conserved in Alba2 (Figure 4B).

Discussion

We have shown that the Alba2 protein, which appears to have diverged toward a novel function in *Sulfolobus* species, is expressed at about 5% of the level of Alba1 in stationary phase cells. Furthermore, Alba2 forms a tight heterodimer with Alba1 that is sufficiently stable to allow its crystallization from a 1:1 mixture of the two proteins. These data suggest strongly that the role of Alba2 in the cell is exerted while in a heterodimeric form with Alba1.

DNA binding by Alba1 has been studied by a number of groups utilizing a variety of techniques. The EM images obtained in the 1980s showed that there appear to be two modes in which Alba can bind to plasmid DNA (Lurz et al., 1986): one in which two DNA duplexes are simultaneously complexed by protein at low to intermediate protein:DNA stoichiometries; and another in which a single DNA duplex is complexed under saturating protein concentrations. The former complex results in DNA condensation, whereas the latter displays little or no compaction of DNA (Lurz et al., 1986). These two nucleoprotein forms probably correspond to the two forms observed by gel retardation at stoichiometries of 12 bp and 6 bp DNA per dimer, respectively (Wardle-

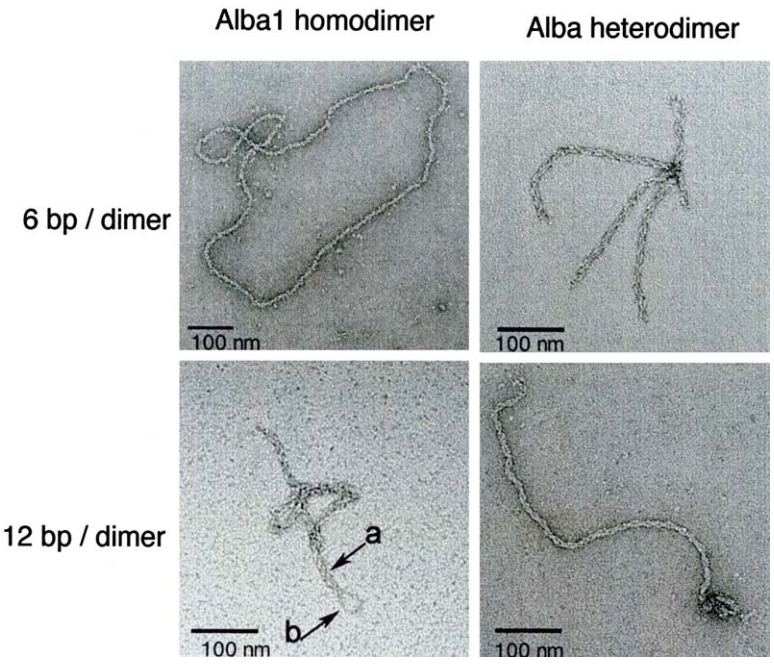

Figure 6. Electron Micrographs of Alba Homo- and Heterodimers Bound to Nicked, Circular phiX174 Plasmid dsDNA

Nucleoprotein filaments formed at DNA:protein ratios of 6 bp/dimer and 12 bp/dimer are shown. The arrows on the bottom left micrograph, where two duplexes are interwound, indicate stem (a) and loop (b) structures.

worth et al., 2002; Xue et al., 2000). The EM data presented here show that the Alba1:Alba2 heterodimer is only able to induce the more highly condensed two-DNA duplex form, and thus may have a role in controlling DNA packaging in vivo.

What is the molecular basis for the differential DNA binding seen for the heterodimer? It is striking from the crystal packing observed in the various crystallographic studies of Alba1 (crystals from three species and five crystal forms) that Alba1 homodimers have a propensity to form filaments via an end-to-end association of dimer units, and it has been suggested that these form the basis of the nucleoprotein filaments observed by EM (Zhao et al., 2003). The interface between Alba1 dimers is highly conserved, suggesting an important conserved function (Zhao et al., 2003). Perhaps significantly, this dimer interface is not well conserved in the Alba2 protein (Figure 4B), and filaments are not observed in either the Alba2 homodimer or Alba1:Alba2 heterodimer crystal lattices.

Duplication of the Alba gene in the *Sulfolobales* has allowed the divergence and specialization of the Alba2 protein, which is expressed at a low level and forms obligate heterodimers with Alba1. These heterodimers may function in a subtle way to "dope" Alba1 filaments, altering their stability and formation kinetics, possibly by changing the stability of the dimer:dimer interface that may, in turn, affect the polymerization of Alba on DNA. This is reflected in the EM observations we have presented, which show differences in the type of DNA compaction observed in the presence of heterodimer. The key point is that gene duplication allows the possibility for differential expression of the two proteins in response to environmental or cellular conditions. An analogous situation has been observed for the histone proteins of the archaeal species *Methanothermus fervidus*, in which the histones HMfA and HMfB are differentially expressed during the growth phase of the organism, with the latter protein providing a greater level of compaction of DNA (Sandman et al., 1994). In eukaryotes, replacement of histone H2A with H2A.Z inhibits the formation of silenced chromatin (reviewed by Owen-Hughes and Bruno (2004). Intriguingly, the Alba ortholog from *Thermococcus zilligi* displays a marked decrease in protein expression level as cells move into stationary phase (Dinger and Musgrave, 2000), and this has also been confirmed by transcript analysis of Alba1 in *Sulfolobus solfataricus* (M. Lundgren and R. Bernander, personal communication). Differential expression of the Alba1 and Alba2 proteins could thus provide a means to modulate chromatin structure in response to environmental or growth conditions.

Experimental Procedures

Cloning, Expression, and Purification of Recombinant Proteins

The Sso10b(2) gene from *Sulfolobus solfataricus* (Alba2) was amplified from genomic DNA by PCR using the primers 5′-CGTCGGATCCCCATGGCAGAAAAATTGAATGAGATAGTAG and 5′-CCGGGGATCCGTCGACTTAGTAAACCCTCTTAAGTCTGAGC. This allows expression of the native protein with a single mutation of threonine to alanine at position 2. The PCR fragment was digested with NcoI and BamHI and cloned into the pET28c expression vector. Recombinant Alba1 and Alba2 were expressed in *E. coli* BL21 *Rosetta* strain and purified as described previously (Wardleworth et al., 2002), with the exception that singly labeled ^{15}N and doubly labeled $^{15}N/^{13}C$ Alba1 proteins were expressed in cell cultures grown in EMBL minimal media containing ^{15}N ammonium sulfate (1 g/l) and/or ^{13}C glucose (2.5 g/l), as appropriate (Goss Scientific Ltd).

Purification of Native Alba Proteins from *Sulfolobus solfataricus*

Sulfolobus solfataricus cell paste (10 g; CAMR, Porton Down) was lysed by sonication in 20 mM Tris (pH 7.5), centrifuged to remove cell debris, and applied to a cation exchange column. Alba proteins were eluted at ~0.5 M NaCl using a 0–1 M gradient. The solution was concentrated to 5 ml and applied to a Superdex-75 gel filtration column and equilibrated in buffer A (20 mM Bis-tris, 0.3 M NaCl, 1 mM azide [pH 6.5]). Fractions containing Alba proteins were pooled and diluted (×10) in buffer B (20 mM Bis-tris, 1 mM azide [pH 6.5]) prior to loading onto a Mono S column. Alba proteins were eluted at ~0.3–0.4 M NaCl using a 0–1 M gradient. Fractions containing Alba proteins were analyzed by SDS-PAGE, Western blot, and MALDI-TOF mass spectrometry.

Protein Concentration Determination

The concentrations of recombinant proteins were calculated using the absorbance at 280 nm. For native Alba1, such measurements tend to overestimate the protein concentration. This is due to the low extinction coefficient of Alba1 at 280 nm ($\epsilon^{0.1\%}_{280nm} = 0.12$). The use of absorbance then becomes error-prone due to relatively large contributions from minor contaminants, leading to a significant overestimation of the true concentration of native Alba1. The crucial difference between the purification of native and recombinant proteins is the heat step, which cannot be effectively used for native proteins. The concentration of Ac-Alba was quantified using a Bradford assay, in which the recombinant Alba1 protein was used for the calibration curve.

Hydroxyapatite Chromatography

A hydroxyapatite column was equilibrated in 5 mM Tris, 1 mM sodium azide (pH 7) prior to loading (1) 200 μl of Alba1 solution at a concentration of ~500 μM, (2) 200 μl of Alba2 at ~200 μM, or (3) 200 μl of an Alba1/Alba2 mixture at a total protein concentration of ~500 μM. Proteins were eluted by applying a linear gradient of sodium phosphate from 0–0.5 M. Fractions having an absorbance were analyzed by SDS-PAGE.

NMR Spectroscopy

The backbone assignment of Alba1 from the sequence identical protein from *Sulfolobus shibatae* (Cui et al., 2003) was used to make a preliminary assignment of the ^{1}H-^{15}N HSQC spectrum of $^{13}C/^{15}N$-labeled Alba1 in 10 mM NaAc, 20 mM KCl, 1 mM NaN_3, 10% D_2O (pH 4.8) at 55°C. The assignment was brought to pH 6.5 by titrating the sample with 1 M disodium phosphate (pH 9). Assignments were verified using a standard set of 3-D experiments (HNCO, HN(CA)CO, HNCA, HNCACB, and CBCA(CO)NH). The titration of Alba1 with Alba2 was performed on a 690 μM solution of ^{15}N-labeled Alba1 in buffer A. The solution was titrated with three aliquots of unlabeled Alba2 to a final molecular ratio of 1:1. After each addition, the solution was equilibrated for ~15 min at 55°C, after which a ^{1}H-^{15}N HSQC spectrum was acquired. Assignments of slow exchange peaks were made on a proximity basis and subsequently checked with a 3-D HNCA spectrum. Spectra were acquired on Bruker DRX spectrometers operating at 500 and 600 MHz, and NMR data were processed and analyzed using FELIX 2000 (Accelrys, San Diego).

EM

A 1 mg/ml solution of relaxed, circular phiX174 (New England Biolabs) was diluted 20-fold into buffer A. Solutions were then prepared with either Alba1 or the heterodimer to give DNA (bp) to protein (dimer) ratios of 6:1 or 12:1 in buffer A. These solutions were diluted 10-fold in distilled water. Samples were applied to glow-discharged carbon-coated grids and stained with 0.75% w/v uranyl formate. Images were recorded at 100 kV on a Philips CM100 EM using a 1024 × 1024 pixel CCD camera.

Table 2. Data Collection and Refinement Statistics

Data Collection		Refinement	
Wavelength (Å)	0.931	Reflections (work set)	42675
Resolution (Å)	36.8–1.7 (1.79–1.7)	Reflections (test set)	2208
R_{merge} (%)[a]	8.7 (48.0)	Resolution (Å)	87.7–1.7
$\langle I/\sigma(I)\rangle$	22.6 (5.2)	R factor (%)[b] work	17.0
Completeness (%)	99.9 (99.9)	R factor (%)[b] free	20.5
Redundancy	10.8	Average *B* value (Å^2)	18.6
		Rmsd bonds (Å)	0.019
		Rmsd angles (°)	1.9

Space group: $P3_121$ ($a = b = 102.8$ Å, $c = 66.6$ Å; 2 dimers per asymmetric unit)
[a] $R_{merge} = \Sigma|I(k) - \langle I\rangle|/\Sigma I(k)$, where $I(k)$ is the value of the kth measurement fo the intensity of a reflection, $\langle I\rangle$ is the mean value of the intensity of that reflection and the summation is over all measurements. Figures in parentheses refer to the highest resolution shell.
[b] R factor = $\Sigma_{hkl}|F_{obs}(hkl) - F_{calc}(hkl)|/\Sigma_{hkl}F_{obs}(hkl)$.

Crystallography

Recombinant Alba1 and Alba2 proteins were mixed in equal proportions to give a final protein concentration of 20 mg/ml in 10 mM Tris-HCl, 100 mM NaCl (pH 7.5). Using the sitting drop vapor diffusion method, heterodimer crystals were obtained within 14 days from a solution containing 4 μl of protein sample and 4 μl of 70% MPD, 100 mM HEPES (pH 7.5). A native data set was collected at 100 K on the ID14-3 Beamline at the European synchrotron radiation facility. Data were collected to 1.7 Å at a wavelength of 0.931 Å using a marCCD detector. The crystal belonged to the trigonal space group $P3_121$ or $P3_221$, with cell dimensions of a = b = 102.8 Å, c = 66.6 Å, α = β = 90°, γ = 120°, and contained two dimers per asymmetric unit. Data were processed using the program MOSFLM and scaled using the program SCALA. The structure was solved by molecular replacement using the program AMORE. The phasing model was derived from superimposing the two homodimer crystal structures (PDB codes 1HOX and 1UDV for Alba1 and Alba2, respectively), using LSQKAB, and then combining to produce a heterodimer. Using this search model and data at 15–3 Å resolution, solutions for two dimers in the asymmetric unit were obtained, with a correlation coefficient of 50.3% and an R factor of 49.7% for the space group $P3_121$. Refinement of the model was achieved using the program REFMAC 5. A test data set, comprising 5% of the total data, was generated randomly and removed in order to assess the refinement process. Following several cycles of rigid body and restrained refinement with model building and the addition of solvent molecules, the R factor was reduced to 17.0% and R_{free} to 20.5%. Crystallographic data and refinement statistics are summarized in Table 2. The coordinates have been deposited with the PDB, accession number 2bky.

Isothermal Titration Calorimetry

Samples of recombinant Alba1 and Alba2 proteins were dialyzed extensively against 20 mM MES, 100 mM potassium glutamate (pH 6.5). A 121 μM solution of Alba1 was titrated into a 10 μM solution of Alba2 at 55°C. Heats of dilution were measured in corresponding blank titrations by injecting Alba1 into buffer and buffer into Alba2. Measurements were made using a VP-ITC instrument and data were processed using the program ORIGIN, supplied by the manufacturer (MicroCal).

DNA Electrophoretic Mobility Shift Assays

The sequence of one complimentary strand used to prepare duplexes of 16 and 39 bp in length were 5′-CGG GCC GCA CGC CGG G-3′ and 5′-CGG GAT ACT CCG AGT ACC AGC ATC AAC TTA GCA CCG AGG-3′, respectively. A 16 bp duplex was chosen because it allows DNA binding by Alba without excessive aggregation under NMR conditions, and a high GC content was chosen to increase the stability of the duplex at elevated temperatures. A 39 bp duplex was chosen as a substrate for binding of multiple dimers of Alba that can be analyzed conveniently by gel electrophoretic retardation. One strand was labeled at the 5′ end with [γ-^{32}P]ATP, and duplex DNA was prepared as described previously (Wardleworth et al., 2002). Protein solutions at concentrations of 1 nM to 40 μM were incubated with 10 nM duplex in buffer A at room temperature (~15 min). Samples were electrophoresed under nondenaturing conditions for 90 min at 130 V in 1× TBE buffer. Gels were dried and exposed to image plates overnight. Gels were visualized using a Fuji FLA-5000 phosphoimager and data were processed using the program Imagegauge. Apparent dissociation constants (K_D) were obtained assuming a two-state model for DNA binding, in which fraction bound = $1/(1 + K_D/[alba])^m$, where the additional exponent, m, was included in order to correct for deviations in slope resulting from cooperativity. It should be emphasized that this apparent K_D is not a true defined dissociation constant. Data-fitting and graphical representations were generated using the program KALIEDOGRAPH (Synergy Software).

Supplemental Data

Supplemental data, including tables, are available at http://www.structure.org/cgi/content/full/13/7/963/DC1/.

Acknowledgments

Thanks to Roger Garrett for the advance provision of the Alba sequences from *Sulfolobus acidocaldarius*, and to Simon Newstead and Alex Theodossis for help with the crystallography. We are grateful to the Biotechnology and Biological Sciences Research Council for financial support. M.F.W. is a Royal Society University Research Fellow.

Received: March 22, 2005
Revised: April 23, 2005
Accepted: April 23, 2005
Published: July 12, 2005

References

Aravind, L., Iyer, L.M., and Anantharaman, V. (2003). The two faces of Alba: the evolutionary connection between proteins participating in chromatin structure and RNA metabolism. Genome Biol. *4*, R64.

Bell, S.D., Botting, C.H., Wardleworth, B.N., Jackson, S.P., and White, M.F. (2002). The interaction of Alba, a conserved archaeal chromatin protein, with Sir2 and its regulation by acetylation. Science *296*, 148–151.

Chou, C.C., Lin, T.W., Chen, C.Y., and Wang, A.H. (2003). Crystal structure of the hyperthermophilic archaeal DNA-binding protein Sso10b2 at a resolution of 1.85 Angstroms. J. Bacteriol. *185*, 4066–4073.

Cui, Q., Tong, Y., Xue, H., Huang, L., Feng, Y., and Wang, J. (2003). Two conformations of archaeal Ssh10b: the origin of its temperature-dependent interaction with DNA. J. Biol. Chem. *278*, 51015–51022.

Dinger, M.E., and Musgrave, D.R. (2000). Identification of archaeal genes encoding a novel stationary phase-response protein. Biochim. Biophys. Acta *1490*, 115–120.

Guo, R., Xue, H., and Huang, L. (2003). Ssh10b, a conserved thermophilic archaeal protein, binds RNA in vivo. Mol. Microbiol. *50*, 1605–1615.

Keeling, P.J., and Doolittle, W.F. (1995). Archaea: narrowing the gap between prokaryotes and eukaryotes. Proc. Natl. Acad. Sci. USA *92*, 5761–5764.

Lurz, R., Grote, M., Dijk, J., Reinhardt, R., and Dobrinski, B. (1986). Electron microscopic study of DNA complexes with proteins from the Archaebacterium *Sulfolobus acidocaldarius*. EMBO J. *5*, 3715–3721.

Marsh, V.L., Peak-Chew, S.Y., and Bell, S.D. (2005). Sir2 and the acetyltransferase, Pat, regulate the archael chromatin protein. Alba. J Biol Chem. *280*, 21122–21128.

Owen-Hughes, T., and Bruno, M. (2004). Molecular biology. Breaking the silence. Science *303*, 324–325.

Sandman, K., Grayling, R.A., Dobrinski, B., Lurz, R., and Reeve, J.N. (1994). Growth-phase-dependent synthesis of histones in the archaeon *Methanothermus fervidus*. Proc. Natl. Acad. Sci. USA *91*, 12624–12628.

Sandman, K., Soares, D., and Reeve, J.N. (2001). Molecular components of the archaeal nucleosome. Biochimie *83*, 277–281.

Wardleworth, B.N., Russell, R.J., Bell, S.D., Taylor, G.L., and White, M.F. (2002). Structure of Alba: an archaeal chromatin protein modulated by acetylation. EMBO J. *21*, 4654–4662.

White, M.F., and Bell, S.D. (2002). Holding it together: chromatin in the archaea. Trends Genet. *18*, 621–626.

Wu, L.J. (2004). Structure and segregation of the bacterial nucleoid. Curr. Opin. Genet. Dev. *14*, 126–132.

Xue, H., Guo, R., Wen, Y., Liu, D., and Huang, L. (2000). An abundant DNA binding protein from the hyperthermophilic archaeon *Sulfolobus shibatae* affects DNA supercoiling in a temperature-dependent fashion. J. Bacteriol. *182*, 3929–3933.

Zhao, K., Chai, X., and Marmorstein, R. (2003). Structure of a Sir2 substrate, Alba, reveals a mechanism for deacetylation-induced enhancement of DNA binding. J. Biol. Chem. *278*, 26071–26077.

Accession Numbers

The coordinates have been deposited with the PDB, accession number 2bky.